2. Chapter 2: Iridium bottom-electrode structure for $Pb(Zr_{0.53}Ti_{0.47})O_3$ (PZT) based capacitors.

2.1 Abstract

We have investigated the structural and electrical properties of sol-gel derived $Pb(Zr,Ti)O_3$ (PZT) thin films deposited on Ir electrode-barrier (Ir/poly-Si/SiO_2/Si). Owing to the interface-controlled growth, highly c-axis oriented perovskite PZT thin films were obtained for the post-deposition annealing temperature of 580 ^oC. Additionally, we found that the ferroelectric properties of IrO_2/PZT/Ir/poly-Si capacitors were remarkably changed by the partial pressure of oxygen during the deposition of IrO_2 top electrodes, which could be due to the enhanced reaction of IrO_2 with PZT by the oxygen ion bombardments. Remanent polarization and coercive field of IrO_2/PZT/Ir/poly-Si capacitor with the top electrodes deposited at P_{O2}=1 mtorr was 20 $\mu C/cm^2$ and 30 kV/cm, respectively, and showed negligible polarization fatigue up to 10^{11} switching repetitions. The leakage current density at a field of 80 kV was 5×10^{-8} A/cm^2.

2.2 Introduction

The development of high-density nonvolatile ferroelectric memories (NvFRAMs) is one of the interesting subjects in fields of memory devices. In a one transistor-one capacitor (1T-1C) NvFRAM cell structure[1], the bottom electrode of the capacitor is directly contacted with poly-Si plug, which in turn is connected to the source/drain of the transistor in the memory cell. Hence, the bottom electrode is required to act as an oxygen diffusion barrier in order to prevent the reaction of oxygen with poly-Si plug at highly oxidizing ambient during the fabrication of ferroelectric film. In addition, $Pb(Zr,Ti)O_3$ (PZT) based high–density NvFRAMs require the bottom electrode of the capacitor to help in eliminating the degradation properties, such as polarization fatigue, aging and retention. Recently, Ir and IrO_2 have attracted attention as electrode materials for PZT thin film capacitors since they showed high quality ferroelectric properties which are comparable to those of Pt/PZT/Pt capacitors. However, most reported PZT capacitors with such electrodes have hybrid electrode structures[2,3,4], such as Pt/IrO_2 and Ir/IrO_2. Since they have more complex processes and relatively large thickness, such electrode structures may be unsuitable for the integration of NvFRAMs. Moreover, if one would try to use such hybrid electrodes as a bottom electrode in the 1T-1C cell structure, the additional layer[5] for oxygen barrier should be needed in order to protect the reaction of oxygen with poly-Si. Hence, the development of a simple and thin electrode-barrier structure is necessary from the practical aspect point of view. Recently, we have successfully prepared the high-quality PZT capacitor having the most simple structure, IrO_2/PZT/Ir/poly-Si, which showed that Ir in itself could act as an electrode-barrier. In this letter, we present the microstructures and electrical properties of PZT thin films

deposited on to Ir/poly-Si substrates. An attempt is made to realize the origin of orientation of PZT thin films during the growth. As a result, we could successfully prepare highly c-axis oriented perovskite rich PZT thin films. In order to characterize the electrical properties of PZT thin film capacitor, we also investigated the effect of top electrodes on their electrical properties.

2.3 Experimental

Ir-layer of 120 nm thickness was deposited onto n+ poly-Si/SiO_2/Si wafers using an rf magnetron sputtering process[5]. The partial pressure of Ar was $2.0x10^{-3}$ torr. The deposition rate of Ir was 10 nm/min. PZT thin films of about 250 nm thickness, with a composition of $Pb_{1.1}(Zr_{0.53}Ti_{0.47})O_3$, were deposited on Ir/poly-Si by means of a conventional sol-gel method[6]. All the electrical measurements were performed by using a two probe contact between the surface of poly-Si and IrO_x top electrode. The IrO_x top electrodes of $3.5\times10^{-4}cm^2$ area and 80 nm thickness were deposited using the rf-reactive sputtering of Ir target in Ar+O_2 ambience. The partial pressure of Ar (P_{Ar}) was fixed at 2 mtorr, but that of O_2 (P_{O2}) was varied from zero to 3 mtorr in order to investigate the optimum deposition conditions of IrO_x top electrode.

The ferroelectric properties, such as P-E hysteresis loop and polarization fatigue were measured using a standard RT66A ferroelectric tester (Radiant Technologies) and also, the fatigue tests were performed using an externally generated square wave with an amplitude of ± 5 V and a frequency of 1 MHz. The dc electrical current-voltage characteristics of these capacitors were measured using an electrometer/source (Keithley 617). X-ray diffraction (XRD) was used to determine the crystallinity of annealed IrO_2 thin films and PZT films. The surface morphologies of PZT films were investigated using an atomic force microscope (AFM).

2.4 Results and Discussion

Figure 2.1 shows the X-ray diffraction (XRD) patterns of PZT/Ir/poly-Si thin films annealed at different temperatures. It could be seen that all PZT thin films annealed at temperatures greater than 560 ^{o}C had perovskite single phase with highly c-axis orientation. However, for annealing temperatures greater than 600 ^{o}C, PZT (011) and (111) peaks appeared in XRD patterns of Fig. 2.1, which were accompanied with small IrO_2 (110) peak at $2\theta=28.4^{o}$. Such IrO_2 peaks could be accompanied by the formation of an amorphous Pb-Ir-O phase formed due to the reaction of Ir with PbO in PZT during annealing process. Work done earlier by our group[7] had shown that PZT thin films processed on as-deposited IrO_2/Ir electrodes possessed random orientation. Additionally, it was also shown that PZT thin films processed on annealed IrO_2/Ir electrodes possessed a greater tendency of c-axis orientation. While our sol-gel derived PZT thin films deposited on a Pt/Ti/SiO_2/Si substrate exhibited highly (111) preferred orientation[6], those deposited on Ir/poly-Si substrates showed highly c-axis orientation. The fact that the orientation of PZT thin films is related to the materials of bottom electrodes implies that the crystallization of PZT thin films on metal electrodes is mainly dominated by the interface-controlled growth. The orientation of PZT thin films on Pt bottom electrode, as reported by many workers, depends strongly on the heating treatments as well as on the deposition methods. Amongst them, Chen and Chen[8] suggested the interface-growth

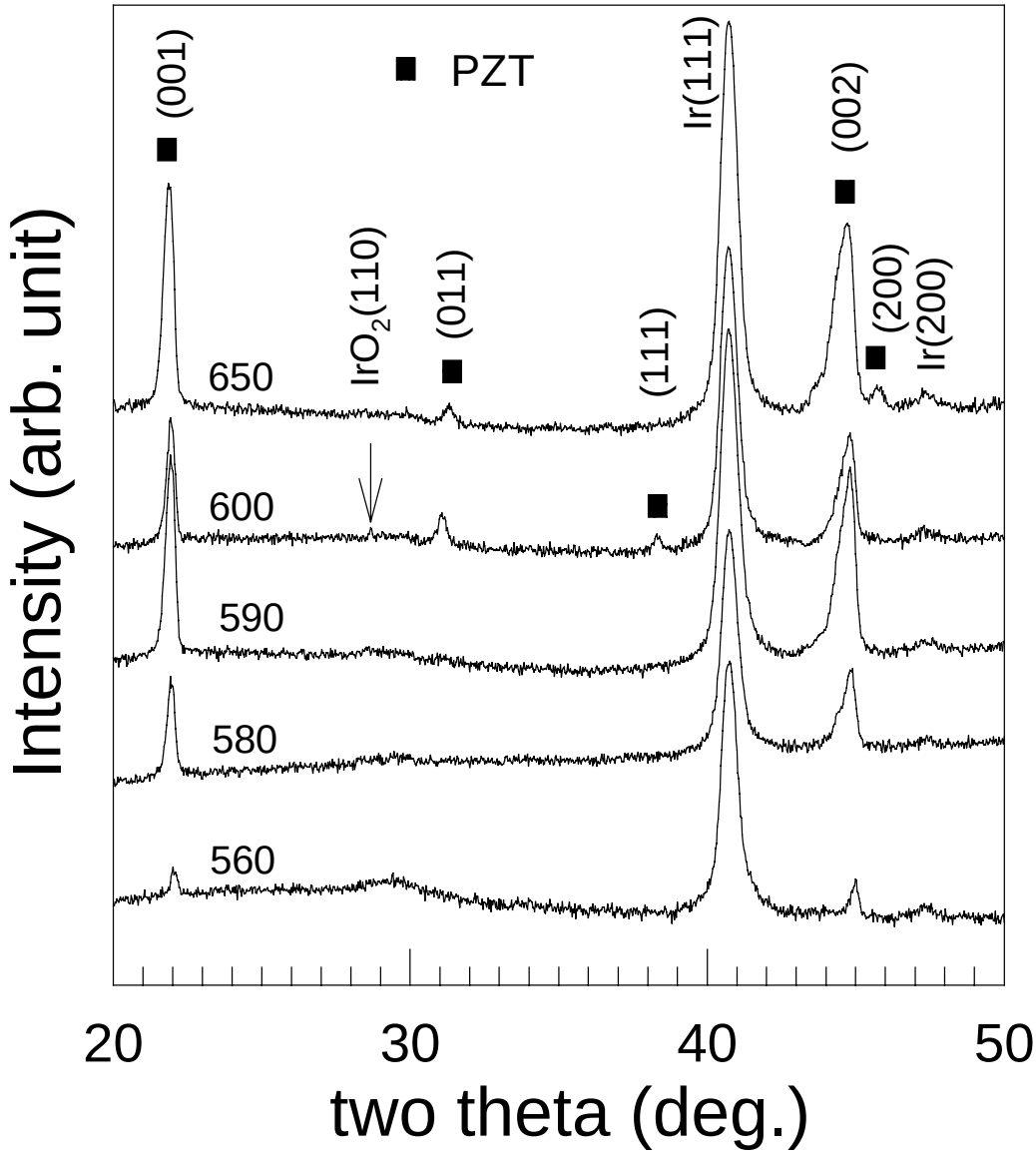

Fig. 2.1 X-ray diffraction patterns of PZT/Ir/poly-Si thin films post-annealed at different temperatures ranging from 560 ^{o}C to 650 ^{o}C.

in PZT, that is, when a (111)- oriented $Pt_{5-7}Pb$ intermetallic phase was formed during the pyrolysis step, it provided the template for the growth of (111)-oriented PZT, while if (001) PbO formed first a (001) PZT orientation was observed since there is a reasonable lattice match between (001) PbO and (001) PZT. In the case of PZT/Ir/poly-Si, amorphous Pb-Ir-O phase was the most possible interfacial phase between PZT and Ir bottom electrodes[9]. Hence, we assumed that highly c-axis oriented PZT on Ir might be due to the preferential growth so as to minimize surface energy, since a (001) texture represented minimum surface energy. On the other hand, if once (111) or (110) IrO_2 phases were formed, growth of PZT might be interfered by solid-phase epitaxial effect resulting in randomly oriented PZT films. However, further investigations would be needed in order to confirm our assumption.

We investigated the fundamental electrical properties, such as P-E hysteresis loop, polarization fatigue behavior and the leakage current-voltage (I-V) characteristics, of highly c-axis oriented PZT thin film capacitors annealed at 580 ^{o}C. The details of the electrical measurement are described elsewhere[5,7]. All the electrical measurements were performed by using a two probe contact between the surface of poly-Si and IrO_x top electrode. The IrO_x top electrodes of $3.5\times10^{-4}cm^2$ area and 80 nm thickness were deposited using the rf-reactive sputtering of Ir target in $Ar+O_2$ ambience. The partial pressure of Ar (P_{Ar}) was fixed at 2 mtorr, but that of O_2 (P_{O2}) was varied from zero to 3 mtorr in order to investigate the optimum deposition conditions of IrO_x top electrode. Figure 2.2 shows the typical P-E hysteresis loops of

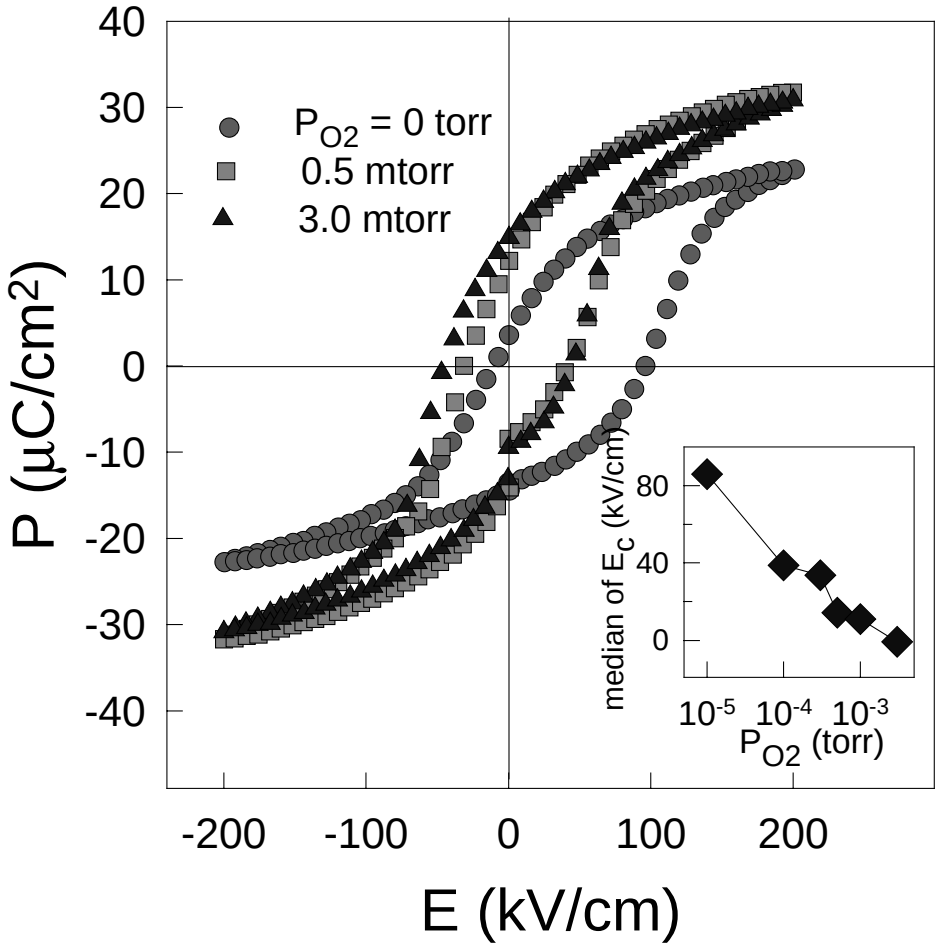

Fig. 2.2. Typical P-E hysteresis loops of IrO_2/PZT/Ir/poly-Si capacitors, where IrO_2 top electrode were sputter-deposited at different oxygen partial pressures, P_{O2}. The inset of this figure shows the plot of median of E_c [=(+E_c)+(-E_c)] *vs.* P_{O2}.

IrO_x/PZT/Ir/poly-Si capacitors with different P_{O2}. It can be seen that as P_{O2} is increased, the symmetry of the P-E hysteresis loop has increased, which is also shown in the inset of Fig. 2.2 as a plot of median between two coercive field ($+E_c$ and $-E_c$) *vs.* P_{O2}. In order to interpret these results, we investigated the compositional ratio of Ir/O in IrO_x with different P_{O2} using ESCA. However, for all IrO_x films deposited with different P_{O2}, the atomic ratios of Ir/O were absolutely same as 32/68, which corresponded to IrO_2. Hence, we thought that the results in Fig. 2.2 might be due to the oxygen ion bombardments during the deposition of top electrodes rather than due to the oxygen contents in IrO_2 top electrodes. As P_{O2} was increased, the oxygen ion bombardments with the PZT/ Ir/poly-Si substrates were increased, which enhanced the reaction of top IrO_2 with PZT. The interfacial states between top IrO_2 electrodes and PZT need to be the same as those between PZT and bottom Ir electrodes in order to obtain a symmetrical P-E hysteresis loop. P_r was about 20 $\mu C/cm^2$ at applied voltages of 5 V (200 kV/cm) and E_c was about 40 kV/cm for PZT capacitors with the top electrode deposited at P_{O2} greater than 0.5 mtorr. Figure 2.3 shows the typical polarization-fatigue behaviors of PZT capacitors with different top electrodes. In Fig. 2.3, the normalized difference between the switched and non-switched polarization (P*-P^) was plotted as a function of switching cycles applied to the capacitors. It could be observed in the inset of Fig. 2.3 that all capacitors with IrO_2 top electrodes deposited at P_{O2} less than 1 mtorr had negligible fatigue loss of around 10 % after 1×10^{11} polarization repetitions. However, PZT capacitor IrO_2 top electrodes

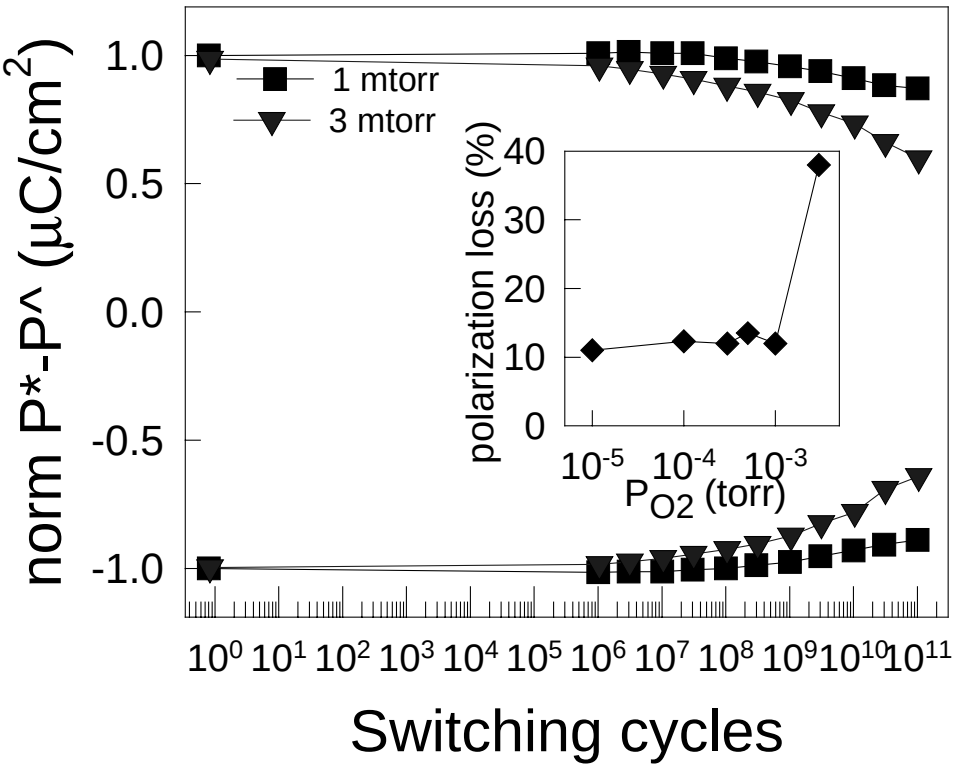

Fig. 2.3. Typical polarization fatigue behaviors of IrO_2/PZT/Ir/poly-Si capacitors having different IrO_2 top electrode deposited at P_{O2}. The inset of these figure shows the plot of polarization loss after 1×10^{11} switching repetitions *vs.* P_{O2}.

deposited at P_{O2}= 3 mtorr exhibited about 40% polarization loss. Such results indicated that excessive reaction of the top electrode with PZT by oxygen ion bombardments could be a cause of defects which might be the origin of polarization fatigue in PZT capacitors. Hence, a well controlled top electrode deposition might enhance the fatigue resistivity of PZT capacitors. Figure 2.4 shows the I-V characteristics of IrO_2/PZT/Ir/poly-Si capacitors with the top electrodes deposited at P_{O2}=1 mtorr. In Fig. 2.4, it could be seen that for fields smaller than 80 kV/cm, the leakage current densities were below 1×10^{-7} A/cm^2. However, above intermediate fields of 80 kV/cm, high leakage current of around 1×10^{-4} A/cm^2 could be seen, which was normally observed for PZT capacitors with high defect concentration, such as for PZT capacitors with conducting oxide electrodes. This suggests that in the IrO_2/PZT/Ir/poly-Si capacitors, the undetected interfacial phase formed at the interface between PZT film and both electrodes might have diminished the microstructure of PZT layer. Hence, there could have been enough defect states in PZT layer which caused the PZT capacitors to be leaky. Such a fact could be confirmed from atomic force microscopic images (2×2 μm^2) of the PZT/Ir/poly-Si surface, as shown in the inset of Fig. 2.4, which showed an appreciable amount of second phase non-uniformly distributed on the surface of PZT layer.

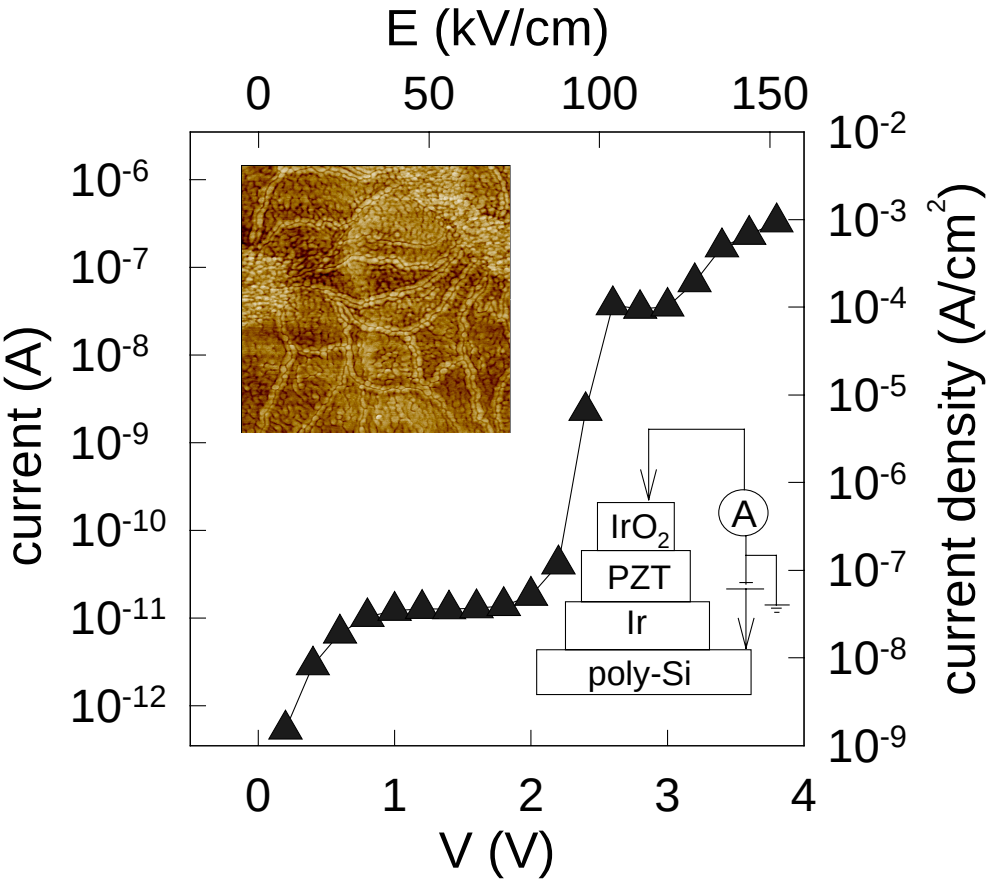

Fig. 2.4. Leakage current-voltage characteristic of IrO_2/PZT/Ir/poly-Si capacitor having IrO_2 top electrode deposited at P_{O2}=1 mtorr. The inset of this figure shows a AFM image (2×2 μm^2) of the surface of PZT/Ir/poly-Si capacitor.

2.5 Conclusions

Conclusively, we have prepared highly c-axis oriented PZT thin films deposited on Ir/poly-Si. The orientation of these films were believed to be controlled by the preferential growth on the interfacial phase of amorphous Pb-Ir-O so as to minimize surface energy. The ferroelectric properties of IrO_2/PZT/Ir/poly-Si capacitor were remarkably changed by the partial pressure of oxygen during the deposition of IrO_2 top electrodes, which was due to the enhanced reaction of IrO_2 with PZT by the oxygen ion bombardments. PZT capacitors with IrO_2 top electrodes deposited at P_{O2} = 1 mtorr exhibited a highly symmetric P-E hysteresis loop with remanent polarization and coercive field of 20 $\mu C/cm^2$ and 30 kV/cm, respectively, and showed lack of polarization fatigue up to 10^{11} switching repetitions. The leakage current densities at a field of 80 kV and 120 kV were 5×10^{-4} A/cm^2 and 1×10^{-4} A/cm^2, respectively. The results of this work proved that Ir in itself could act as an bottom electrode-barrier for PZT capacitor. If one could reduce the interfacial phases between PZT and electrodes, the leakage current behaviors would further improve and high quality IrO_2/PZT/Ir/poly-Si capacitors with a simple electrode-barrier structure could be fabricated for high density NvFRAMs.

References

1. R. Rameshi, W. K. Chan, B. Wiikens, H. Gilchrist, T. Sands, J. M. Tarascon, V. G. Keramdas, D. K. Fork, J. Lee, and A. Safari, Appl. Phys. Lett. **61**, 1537(1992).

2. T. Nakamura, Y. Nakao, A. Kamisawa and H. Takasu, Appl. Phys. Lett. **65**, 1522(1994).

3. T. Nakamura, Y. Nakao, A. Kamisawa and H. Takasu, Jpn. J. Appl. Phys. **34**, 5184(1995).

4. M. Shimizu, H. Okino, H. Fujisawa and T. Shiosaki, ISAF (1996) Proc. IEEE Int. Symp. Appl. Ferroelectrics **10,** 471.

5. K. B. Lee, Y. Song, S. Tirumala and S. B. Desu, Appl Phys. Lett. (1998) unpublished.

6. Y. Song, Y. Zhu, and S. B. Desu, Appl. Phys. Lett. **72**, 2686(1998).

7. K. B. Lee, S. Tirumala and S. B. Desu, J. Mater. Res. (1998) unpublished.

8. S. Y. Chen and I. W. Chen, J. Am. Ceram. Soc. **77**, 2332(1994).

9. M. Shimizu, H. Fujisawa, S. Hyodo, S. Nakashima, H. Niu, H. Okino and T. Shiosaki, *Ferroelectric Thin Films IV*, (Mater. Res. Soc. Symp. Proc. **493**, Boston, 1997) p. 159.